obtained from the Physical Sciences Division of Earth System Research Laboratory, National Oceanic and Atmospheric Administration (NOAA).

Our focus here is to apply an advanced method, the self-organizing map (SOM), to re-examine the long-term satellite observations archived for the LC region in the last two decades. Actually, satellite data have been widely used in studying the Gulf circulation and LC dynamics (e.g., Leben 2005; Leben and Honaker 2006; Lugo-Fernández and Leben 2010). Based on an unsupervised artificial neural network, the SOM is an effective method for feature extraction and classification, and can map high-dimensional input data onto the elements of a regular, low-dimensional array (Kohonen 2001). It has been demonstrated to be more powerful than the conventional empirical orthogonal function method for feature extractions, especially when the signal is highly nonlinear (Reusch, Alley, and Hewitson 2005; Liu, Weisberg, and Mooers 2006). The SOM has been shown to be a valuable tool in oceanographic studies (Liu and Weisberg 2011). It has been applied to identify patterns in ocean currents and sea surface temperature fields on the West Florida Shelf (Liu and Weisberg 2005; Liu, Weisberg, and He 2006; Liu, Weisberg, and Shay 2007), biogeochemical properties in the northern Adriatic Sea (Solidoro et al. 2007) and current variability in the China Seas (Liu, Weisberg, and Yuan 2008; Jin et al. 2010; Tsui and Wu 2012; Yin et al. 2014).

In this study, all weekly SSH data within the study domain were fed into the SOM as inputs. Based on the minimum Euclidean distance and pattern size given initially, different SSH patterns were extracted in a topology-preserving way. Each weekly SSH snapshot was then assigned to one of these patterns (e.g., Liu and Weisberg 2005). From these assignments, the best matching unit (BMU) time series and FO of each pattern were obtained. The SOM parameters such as lattice, weights, training method and neighbourhood function were chosen according to Liu, Weisberg, and Mooers (2006). Based on our sensitivity experiments and the variability of the LC, the pattern number 1×3 with contrasting difference between each pattern was chosen prior to the training process.

3. Results

3.1. Spatial variability

The three SOM patterns and their corresponding FOs are shown in Figure 2. The 0.45 m SSH contour line was chosen as the edge of the LC and its detached eddies in this study, based on the examination of patterns and evolutions of LC and LC eddies over 21 years SSH data record. It is consistent with methods used by earlier studies (e.g., Leben 2005) in SSH contour selection. As shown in Figure 2(*a*), Pattern 1 (P1) is the LC's normal condition, without extension or shedding. The north and west edges of LC in P1 reach about 26.5°N and 88°W, respectively. For P1, the LC is featured with significantly high sea level, accompanied by low sea level on the north-west edge. Pattern 2 (P2) is the LC extension pattern. The most obvious feature for P2 is that the LC extends into a relatively elongated shape, such that its north and west edges reach about 27.5°N and 90°W. In contrast, Pattern 3 (P3) represents the LC retraction pattern, which can also be considered as the eddy shed pattern. The main body of the LC and LC eddy are clearly separated from each other. After eddy shedding, the north and west edges of the LC retreat to about 25.5°N and 86°W. The shed eddy is located at about 26°N, 90°W with lower SSH and weaker geostrophic velocity than the main LC. Different from P1 and P2, P3 shows the LC further to the south-east after eddy shedding. There is also a large cyclonic eddy with low SSH present between the LC and its shed eddy.

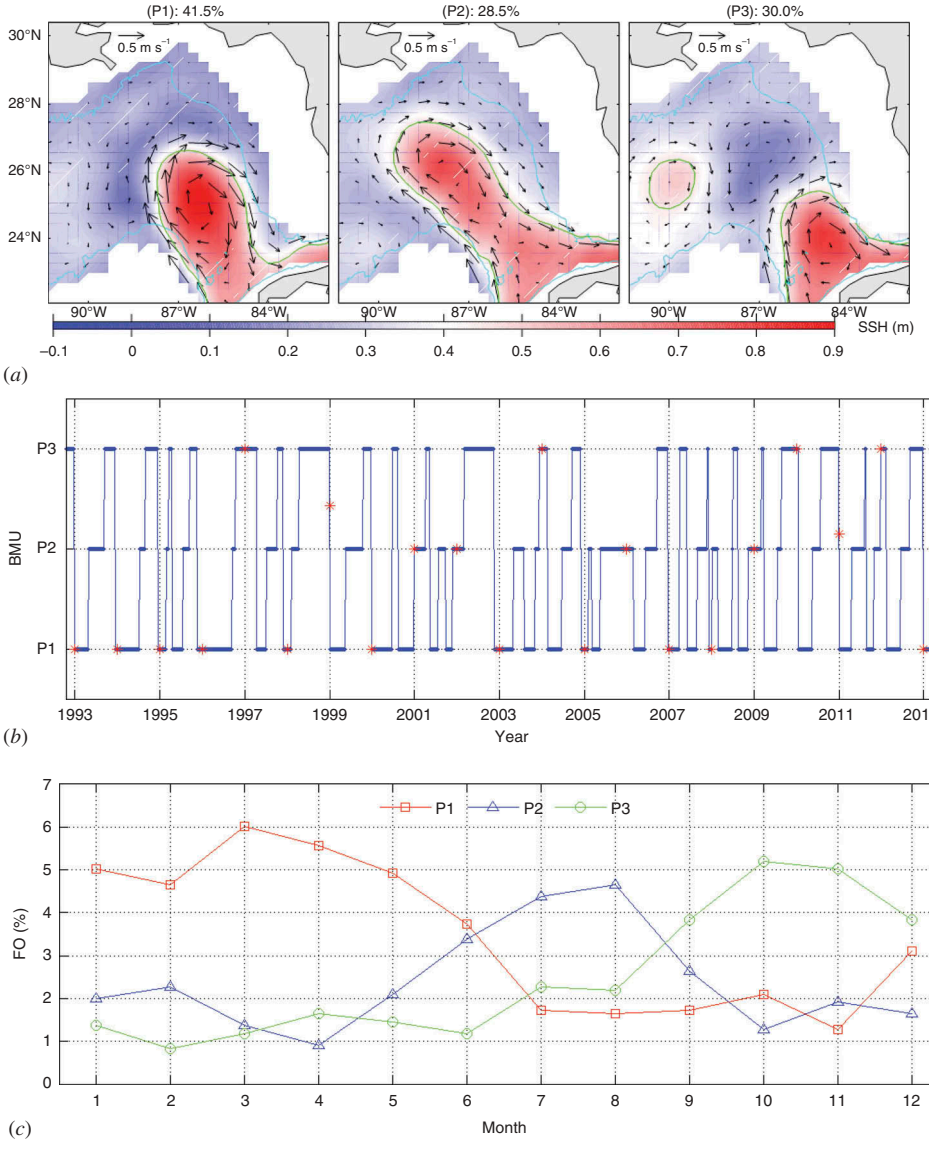

Figure 2. SOM analysis results. (*a*) SSH patterns: (P1) normal; (P2) extension; (P3) retraction. Top numbers are corresponding FO percentage. Vectors are geostrophic current. Green line is 0.45 m SSH contour line. Cyan lines are 1000 m isobaths. Colour scale: SSH in metres. (*b*) BMU time series of the three patterns in (*a*). Red stars are the first day of each year. (*c*) Monthly FOs of the three patterns in (*a*).

3.2. *Temporal evolution*

Figure 2(*b*) shows the temporal changes (BMU time series) of the three LC patterns (P1, P2 and P3). A repeated cycle is generally evident in the 21-years' time series. Using P1 as an arbitrary beginning, the cycle of P1→P2→P3→P1 is fairly robust. Specifically, the LC starts in its normal pattern (P1), and then extends to the north-west to 27.5°N to reach its extension pattern (P2). An eddy shedding event subsequently occurs, and then the LC

retreats to about 25.5°N to its retraction pattern (P3). However, due to the nonlinearity associated with LC flow and vorticity dynamics (e.g., Lugo-Fernández 2007), not every warm eddy shedding process follows this cycle. In a few events (e.g., in 2005), there was no eddy separation followed by a proceeding extension pattern. In several other events (e.g., in 2008), the eddy separation pattern occurred right after the normal pattern, bypassing the extension pattern

In order to quantify the percentage occurrence of each pattern, the FO was calculated by summing the number of occurrences of that pattern divided by the total record length. Over the 21-year study period, 41.5% of the LC patterns belong to the normal pattern (P1), while the extension (P2) and retraction (P3) patterns account for 28.5% and 30.0%, respectively. To better illustrate the seasonal variation of the LC and the dominant pattern for each month, the monthly FOs (MFO) of the three patterns were also calculated (Figure 2(*c*)). The MFO of P1 is larger than those of P2 and P3 from January to May, which suggests that generally the LC tends to remain in its normal pattern (P1) during this period. In July and August, the MFO of P2 is the largest, suggesting that LC tends to extend during this period. The MFO of P3 becomes dominant from September to December, showing that retraction of the LC is more likely to occur during this period. We note that transitions from P1 to P2 and from P2 to P3 occur in June and the end of August, respectively, indicating that statistically the LC extension (eddy shedding) tends to occur in June (in late August).

4. Discussion

To further study the LC eddy shedding process and its possible mechanisms, we compared the weekly and annual FOs of P3 with long-term mean wind stress curl (WSC) over different spatial domains, as well as with different climate indices.

Figure 3(*a*) shows the weekly FO (WFO) of P3 along with long-term weekly mean WSC of three (Caribbean Sea, Bahamas and GoM; see Figure 1) previously identified wind influence regimes (e.g., Oey, Lee, and Schmitz 2003; Sturges, Hoffmann, and Leben 2010; Gopalakrishnan, Cornuelle, and Hoteit 2013). We found that the zero time lag correlation coefficient between CS WSCs and WFO of P3 is 0.83, much higher than the correlations with the local WSC in the GoM (correlation coefficient $r = 0.45$) and the downstream WSC in the Bahamas area ($r = 0.65$). This suggests that LC eddy shedding is likely associated more with CS WSC in the upstream Caribbean Sea. Indeed, Oey, Lee, and Schmitz (2003) showed that negative CS WSC can spin up Caribbean eddies (anticyclones), which in turn lead to a lower frequency of LC shedding. Our results further reveal the CS WSC increases from June to November. It can play a role in suppressing the formation of anti-cyclonic eddies in the CS. In other words, the increase of CS WSC during this period favours a higher frequency of LC shedding, as shown in Figure 3(*a*).

To understand the interannual variability of LC eddy shedding, the annual FO (AFO) of P3 was examined together with various climate indices, including the ONI, North Atlantic Oscillation index (NAO), Southern Oscillation Index (SOI) and Pacific Decadal Oscillation (PDO). Various time lag correlations and running averages were performed. Among them, the best correlation ($r = 0.6$ at 95% confidence interval) is found between the six-month moving-averaged ONI and the AFO of P3 with a 90-day lag (Figure 3(*b*)). Other indices show no significant correlations (not shown). The ONI is defined as the sea surface temperature anomalies in Niño Region 3.4 (5°N–5°S, 120°W–170°W) and used as an index for El Niño (e.g., Kousky and Higgins 2007). The relationship between ONI and AFO of P3 suggests a possible connection between Pacific climate and the LC eddy shedding process.

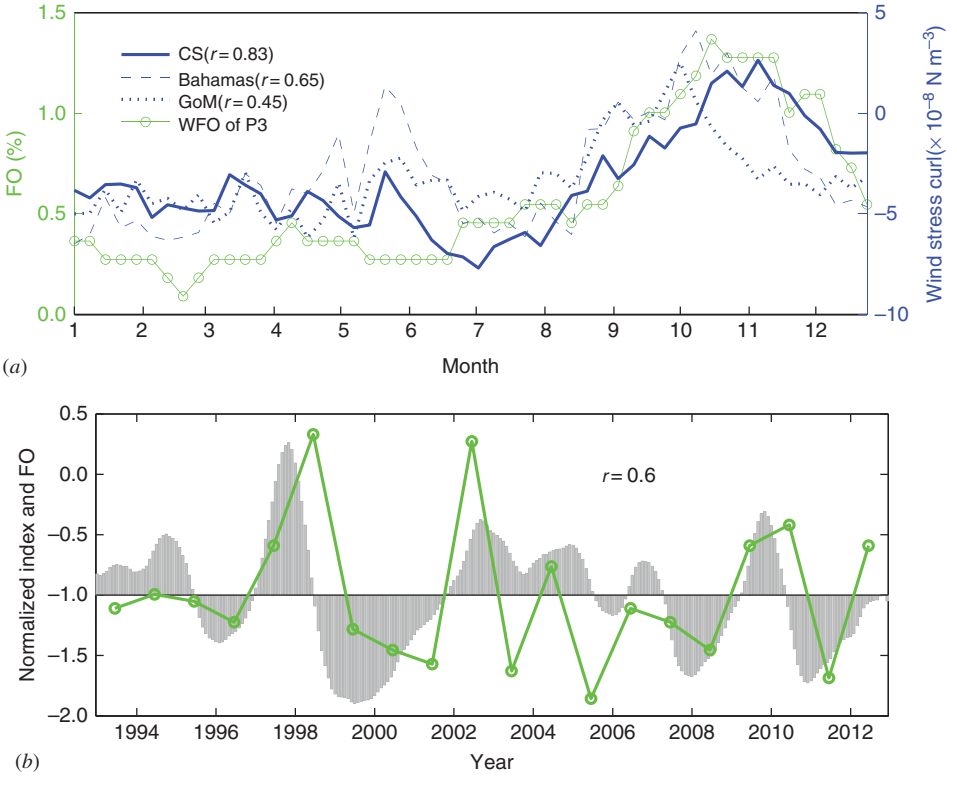

Figure 3. (*a*) Weekly frequency of occurrence (WFO) for Pattern 3 (P3) and WSC of the areas in Figure 1. Zero-lag correlation coefficients (*r*) for the relation between the WFO of P3 and the WSC, at 95% confidence level for each domain, are shown in brackets after the domain. (*b*) Normalized Oceanic Niño Index (ONI) (6-months moving average; shaded area) and annual mean FO for P3 (green line). Correlation coefficient ($r = 0.6$) with ONI lagged 90 days are shown at 95% confidence interval.

Previous studies on the teleconnection between the Atlantic and the Pacific showed that El Niño, a Pacific event, can have a strong impact on wind and circulation in the Atlantic (Enfield and Mayer 1997; Alexander and Scott 2002; Kennedy et al. 2007; Smith et al. 2007). The frequent swing in the trade winds and resulting WSCs in the Atlantic may favour more eddy shedding in the GoM (Chang and Oey 2013b). Detailed processes determining how the basin-scale teleconnection influences LC eddy shedding clearly need further study that combines observations and numerical model sensitivity experiments.

5. Summary

Three patterns and corresponding temporal evolution of LC SSH were extracted from 21 years of weekly satellite SSH data using the SOM method. In most cases, the LC evolution follows a normal–extension–retraction cycle. Transitions from normal pattern (P1) to extension pattern (P2) and from extension pattern (P2) to retraction pattern (P3) occur in June and the end of August, respectively.

The weekly FO analysis of the LC retraction pattern (P3) indicates CS WSC has a major influence on LC eddy shedding. The increase of CS WSC from June to November favours the LC eddy shedding at higher frequency during that period. On the interannual time scale, the significant relationship between ONI and AFO of P3 suggests a possible connection between Pacific climate and LC eddy shedding frequency, which needs further study. Due to the fully three-dimensional nature of the LC and its high nonlinearity (e.g., Lugo-Fernández 2007), realistic dynamical modelling study is needed to better understand causes of LC shedding, vertical structure of circulation, as well as their responses to various forcing agents and climate signals.

Acknowledgements

The authors would like to acknowledge the Helsinki University of Technology, Finland for providing the SOM Toolbox and Dr. Y. Liu of University of South Florida for useful guidance on the SOM application in oceanography. Constructive comments provided by two anonymous reviewers and J. Warrillow's editorial assistance are also appreciated.

Funding

Research support provided by Gulf of Mexico Research Initiative/GISR [grant number 02-S130202]; NOAA [grant number NA11NOS0120033]; NASA [grant number NNX12AP84G], [grant number NNX13AD80G] is much appreciated.

References

Alexander, M., and J. Scott. 2002. "The Influence of ENSO on Air-Sea Interaction in the Atlantic." *Geophysical Research Letters* 29 (14): 46. doi:10.1029/2001GL014347.

Chang, Y.-L., and L.-Y. Oey. 2012. "Why Does the Loop Current Tend to Shed More Eddies in Summer and Winter?" *Geophysical Research Letters* 39 (5): L05605. doi:10.1029/2011GL050773.

Chang, Y.-L., and L.-Y. Oey. 2013a. "Loop Current Growth and Eddy Shedding Using Models and Observations: Numerical Process Experiments and Satellite Altimetry Data." *Journal of Physical Oceanography* 43 (3): 669–689. doi:10.1175/JPO-D-12-0139.1.

Chang, Y.-L., and L.-Y. Oey. 2013b. "Coupled Response of the Trade Wind, SST Gradient, and SST in the Caribbean Sea, and the Potential Impact on Loop Current's Interannual Variability." *Journal of Physical Oceanography* 43 (7): 1325–1344. doi:10.1175/JPO-D-12-0183.1.

Cushman-Roisin, B., and J.-M. Beckers. 2011. *Introduction to Geophysical Fluid Dynamics: Physical and Numerical Aspects*. Waltham, MA: Academic Press.

Enfield, D. B., and D. A. Mayer. 1997. "Tropical Atlantic Sea Surface Temperature Variability and Its Relation to El Niño-Southern Oscillation." *Journal of Geophysical Research: Oceans* 102 (C1): 929–945. doi:10.1029/96JC03296.

Gopalakrishnan, G., B. D. Cornuelle, and I. Hoteit. 2013. "Adjoint Sensitivity Studies of Loop Current and Eddy Shedding in the Gulf of Mexico." *Journal of Geophysical Research: Oceans* 1–21. doi:10.1002/jgrc.20240.

Hurlburt, H. E., and J. D. Thompson. 1980. "A Numerical Study of Loop Current Intrusions and Eddy Shedding." *Journal of Physical Oceanography* 10 (10): 1611–1651. doi:10.1175/1520-0485(1980)010<1611:ANSOLC>2.0.CO;2.

Jin, B., G. Wang, Y. Liu, and R. Zhang. 2010. "Interaction Between the East China Sea Kuroshio and the Ryukyu Current as Revealed by the Self-organizing Map." *Journal of Geophysical Research: Oceans* 115: C12047. doi:10.1029/2010JC006437.

Kennedy, A. J., M. L. Griffin, S. L. Morey, S. R. Smith, and J. J. O'Brien. 2007. "Effects of El Niño–Southern Oscillation on Sea Level Anomalies Along the Gulf of Mexico Coast." *Journal of Geophysical Research: Oceans* 112 (C5): C05047. doi:10.1029/2006JC003904.

Kohonen, T. 2001. *Self-Organizing Maps*. New York: Springer.
Kousky, V. E., and R. W. Higgins. 2007. "An Alert Classification System for Monitoring and Assessing the ENSO Cycle." *Weather and Forecasting* 22: 353–371. doi:10.1175/WAF987.1.
Le Hénaff, M., V. H. Kourafalou, Y. Morel, and A. Srinivasan. 2012. "Simulating the Dynamics and Intensification of Cyclonic Loop Current Frontal Eddies in the Gulf of Mexico." *Journal of Geophysical Research: Oceans* 117 (C2): C02034. doi:10.1029/2011JC007279.
Leben, R. R. 2005. "Altimeter-Derived Loop Current Metrics." In *Circulation in the Gulf of Mexico: Observations and Models*, edited by W. Sturges, and A. Lugo-Fernandez, 181–201. Washington, DC: American Geophysical Union.
Leben, R. R., and D. J. Honaker. 2006. "What Do We Know and What Can We Predict About the Timing of Loop Current Eddy Separation?" *ESA Special Publication* 614: 19. http://adsabs.harvard.edu/abs/2006ESASP.614E.19L.
Lee, H.-C., and G. L. Mellor. 2003. "Numerical Simulation of the Gulf Stream System: The Loop Current and the Deep Circulation." *Journal of Geophysical Research: Oceans* 108 (C2): 25. doi:10.1029/2001JC001074.
Liu, Y., S. K. Lee, B. A. Muhling, J. T. Lamkin, and D. B. Enfield. 2012. "Significant Reduction of the Loop Current in the 21st Century and Its Impact on the Gulf of Mexico." *Journal of Geophysical Research: Oceans* 117 (C5). doi:10.1029/2011JC007555.
Liu, Y., and R. H. Weisberg. 2005. "Patterns of Ocean Current Variability on the West Florida Shelf Using the Self-organizing Map." *Journal of Geophysical Research: Oceans* 110 (C6): C06003. doi:10.1029/2004JC002786.
Liu, Y., and R. H. Weisberg. 2011. "A Review of Self-Organizing Map Applications in Meteorology and Oceanography." In *Self Organizing Maps – Applications and Novel Algorithm Design*, edited by J. I. Mwasiagi. Croatia: InTech.
Liu, Y., R. H. Weisberg, and R. He. 2006. "Sea Surface Temperature Patterns on the West Florida Shelf Using Growing Hierarchical Self-Organizing Maps." *Journal of Atmospheric and OceanicTechnology* 23 (2): 325–338.
Liu, Y., R. H. Weisberg, and C. N. K. Mooers. 2006. "Performance Evaluation of the Self-organizing Map for Feature Extraction." *Journal of Geophysical Research: Oceans* 111 (C5): C05018. doi:10.1029/2005JC003117.
Liu, Y., R. H. Weisberg, and L. K. Shay. 2007. "Current Patterns on the West Florida Shelf from Joint Self-Organizing Map Analyses of HF Radar and ADCP Data." *Journal of Atmospheric and Oceanic Technology* 24 (4): 702–712. doi:10.1175/JTECH1999.1.
Liu, Y., R. H. Weisberg, and Y. Yuan. 2008. "Patterns of Upper Layer Circulation Variability in the South China Sea from Satellite Altimetry Using the Self-Organizing Map." *Acta Oceanologica Sinica* 27 (Supp.): 129–144.
Lugo-Fernández, A. 2007. "Is the Loop Current a Chaotic Oscillator?" *Journal of Physical Oceanography* 37 (6): 1455–1469. doi:10.1175/JPO3066.1.
Lugo-Fernández, A., and R. R. Leben. 2010. "On the Linear Relationship Between Loop Current Retreat Latitude and Eddy Separation Period." *Journal of Physical Oceanography* 40 (12): 2778–2784. doi:10.1175/2010JPO4354.1.
Maul, G. A., and F. M. Vukovich. 1993. "The Relationship between Variations in the Gulf of Mexico Loop Current and Straits of Florida Volume Transport." *Journal of Physical Oceanography* 23 (5): 785–796. doi:10.1175/1520-0485(1993)023<0785:TRBVIT>2.0.CO;2.
Nürnberg, D., M. Ziegler, C. Karas, R. Tiedemann, and M. W. Schmidt. 2008. "Interacting Loop Current Variability and Mississippi River Discharge over the Past 400 Kyr." *Earth and Planetary Science Letters* 272 (1–2): 278–289. doi:10.1016/j.epsl.2008.04.051.
Oey, L.-Y., and Y.-L. Chang. 2011. "Loop Current Cycle and Trigger Mechanism for Loop Current Ring Separations." In *Proceedings of the BOEMRE Information Transfer Meeting*, New Orleans, LA, edited by M. Mckay and J. Nides, 30–36. New Orleans, LA: U.S. Dept. of the Interior, Bureau of Ocean Energy Management, Gulf of Mexico OCS Region.
Oey, L.-Y., T. Ezer, and H.-C. Lee. 2005. "Loop Current, Rings and Related Circulation in the Gulf of Mexico: A Review of Numerical Models and Future Challenges." In *Circulation in the Gulf of Mexico: Observations and Models*, edited by W. Sturges, and A. Lugo-Fernandez, 31–56. Washington, DC: American Geophysical Union.
Oey, L.-Y., H.-C. Lee, and W. J. Schmitz. 2003. "Effects of Winds and Caribbean Eddies on the Frequency of Loop Current Eddy Shedding: A Numerical Model Study." *Journal of Geophysical Research: Oceans* 108 (C10): 22. doi:10.1029/2002JC001698.

Pichevin, T., and D. Nof. 1997. "The Momentum Imbalance Paradox." *Tellus A* 49 (2): 298–319. doi:10.1034/j.1600-0870.1997.t01-1-00009.x.

Reusch, D. B., R. B. Alley, and B. C. Hewitson. 2005. "Relative Performance of Self-Organizing Maps and Principal Component Analysis in Pattern Extraction from Synthetic Climatological Data." *Polar Geography* 29 (3): 227–251. doi:10.1080/789610199.

Smith, S. R., J. Brolley, J. J. O'Brien, and C. A. Tartaglione. 2007. "ENSO's Impact on Regional U.S. Hurricane Activity." *Journal of Climate* 20 (7): 1404–1414. doi:10.1175/JCLI4063.1.

Solidoro, C., V. Bandelj, P. Barbieri, G. Cossarini, and S. Fonda Umani. 2007. "Understanding Dynamic of Biogeochemical Properties in the Northern Adriatic Sea by Using Self-Organizing Maps and K-Means Clustering." *Journal of Geophysical Research: Oceans* 112: C07S90. doi:10.1029/2006JC003553.

Sturges, W., N. G. Hoffmann, and R. R. Leben. 2010. "A Trigger Mechanism for Loop Current Ring Separations." *Journal of Physical Oceanography* 40 (5): 900–913. doi:10.1175/2009JPO4245.1.

Tsui, I.-F., and C.-R. Wu. 2012. "Variability Analysis of Kuroshio Intrusion Through Luzon Strait Using Growing Hierarchical Self-organizing Map." *Ocean Dynamics* 62 (8): 1187–1194. doi:10.1007/s10236-012-0558-0.

Xu, F.-H., Y.-L. Chang, L.-Y. Oey, and P. Hamilton. 2013. "Loop Current Growth and Eddy Shedding Using Models and Observations: Analyses of the July 2011 Eddy-Shedding Event." *Journal of Physical Oceanography* 43 (5): 1015–1027. doi:10.1175/JPO-D-12-0138.1.

Yin, X.-Q., and L.-Y. Oey. 2007. "Bred-ensemble Ocean Forecast of Loop Current and Rings." *Ocean Modelling* 17 (4): 300–326. doi:10.1016/j.ocemod.2007.02.005.

Yin, Y., X. Lin, Y. Li, and X. Zeng. 2014. "Seasonal Variability of Kuroshio Intrusion Northeast of Taiwan Island as Revealed by Self-Organizing Map." *Chinese Journal of Oceanology and Limnology* 32: 1435–1442. doi:10.1007/s00343-015-4017-x.